Stability of Self-Assembling Drug Amphiphiles in Biological Environments

by

Yuzhu Wang

A dissertation submitted to Johns Hopkins University in conformity with the requirements for the degree of Master of Science in Engineering

Johns Hopkins University

Baltimore, MD 21218

October 2017

Abstract

Chair of Advisory Committee: Dr. Honggang Cui & Dr. David Gracias

The search of understanding the interaction of self-assembling nanostructures with proteins in biological environments is leading to the rapid development of key applications, including improved drug delivery systems with long retention time, and the reduced of nonspecific protein adsorbance of nanoparticles with tuned surface charges. In this work, the self-assembly and the behavior of drug amphiphiles with different charges in the presence of proteins were studied. These prodrug molecules of different surface chemistries are able to assemble into tubular nanostructures in aqueous solution with a similar range of critical micelle concentration(CMC). Among all these drug amphiphiles, non-ionic peptide-drug conjugates exhibit the strongest stability in FBS and human serum while cationic molecules immediately precipitated out in biological environments and other charged nanostructures showed unobvious degradation after two weeks in the presence of protein. We believe these findings build foundation to further study rational design of supramolecular drug amphiphiles for therapeutic issues.

Acknowledgments

First of all, I would like to express my gratitude to my parents for providing me endless amounts of love and unconditional support, and encouraging me to stick on my way and pursue my dream at Johns Hopkins University. They teach me to be independent and to have my own opinions and thoughts, instead of going along with everyone else or following the popular idea.

Then I want to thank my advisor, Dr. Honggang Cui, who gives me a priceless opportunity to gain a scientific perspective and expand my knowledge in his lab. I appreciate that he always has an open-door policy and despite being busy he takes time mentoring me not only to come up with innovative project ideas, but also to author comprehensive reports on data findings, project analysis and project results.

Finally, I would like to show my gratitude to group members in Cui lab: Hao taught me to get hands-on experiences of doing bench work and helped me a lot in cryo-TEM imaging. Yin, Yi, Feihu and Lisi assisted me in solving all kinds of problems in experiments.

Table of Contents

List of Figures and Tables

1. Introduction

The design of peptide-drug conjugates was originally intended to take advantage of short hydrophilic peptides in order to enhance the solubility and to provide additional functionality, such as the use of cell-penetrating peptides and tumor-targeting peptides [1-5]. However, the conjugation of hydrophobic drugs with a low molecular weight and hydrophilic peptide segments can generate overall ampiphilicity, leading to a tendency for self-aggregation in aqueous media. This unintentional conjugation-induced assembly is now receiving rapidly growing interest in the drug delivery community. A class of self-assembling peptide-drug conjugated was recently developed in a way to functionally mimic protein-drug conjugated, termed "drug amphiphiles" (DAs), formed by the covalent conjugation of anticancer drugs to rationally designed peptides via a biodegradable linker [7-12].

1.1 Supramolecular hydrogels formed by self-assembling drug amphiphiles

Hydrogels, three dimensional polymer or supramolecular polymer networks, are an important class of biomaterials for drug delivery due to their sustained drug release capabilities. Early phase of the research in this field focused on polymer-based hydrogels formed by chemical cross-linking[13-18]. A large amount of cross-linking methods have been adapted for hydrogel synthesis and have received extensive attention[19-23]. However, the initiators utilized for hydrogel formation are potentially toxic and need to be removed afterwards. The another obstacle is the degradation of these covalently linked hydrogels in a biological setting, although there have been some novel methods to address this issue, such as incorporating enzymatically degradable or hydrolysable linkages into the systems[24-33]. Hydrogels fabricated by physical entanglement have receive increasing attention[34-37], especially in context of peptide assembly. The existing non-covalent interactions such as van der Waals, hydrogel

bonds, electrostatic interactions, metal-ligand interactions, host-guest recognition, and other types of enthalpic contribution result in the formation of these kind of hydrogels[34-37] (Fig. 1A). In addition, the gelation process is often reversible and can experience a repetitive transition from solution to gel and gel to solution by alternating the solution pH, ionic strength, or temperature (Fig. 1B).

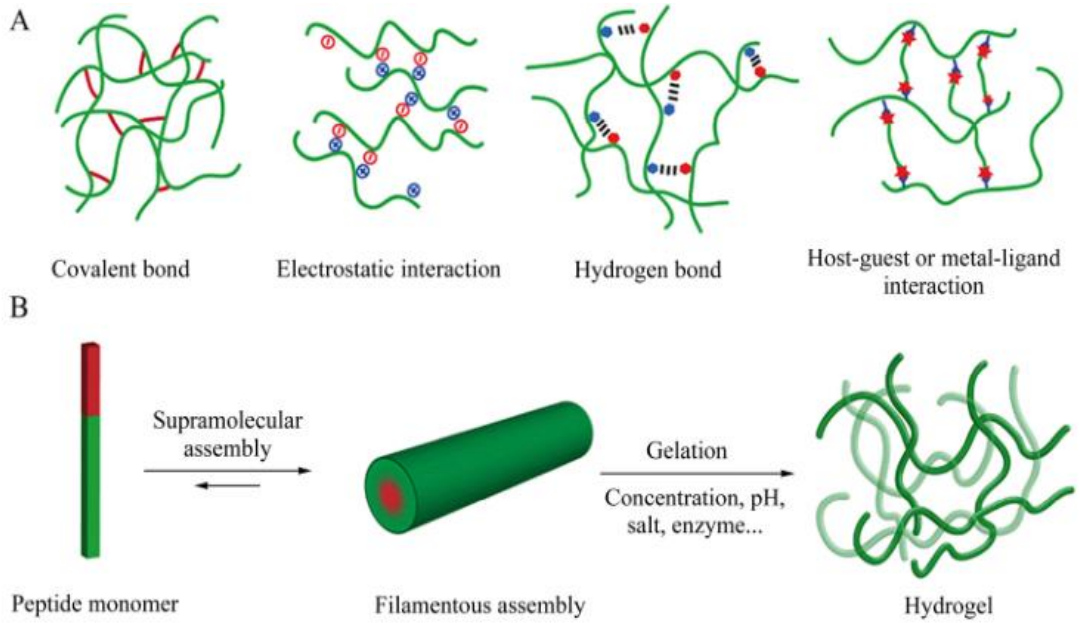

Fig. 1 Schematic illustration of (A) the interaction mechanisms of forming chemically and physically crosslinked polymeric hydrogels: covalent bond, electraostatic interaction, hydrogen bond, and host-guest or metal-ligand interaction, (B)assembly of peptidic monomers into filamentous assemblies that entangle further into supramolecular hydrogels (Reprinted with permission from Ref. [57]; Copyright (2017) Chinese Journal of Polymer Science).

Small molecule peptides or rationally designed peptide derivatives often sever as peptide-based gelators which are prone to assemble into filamentous nanostructures in aqueous solutions [10-11,35,38]. Both molecular and intermolecular interactions at multiple length scales result in gelation. The directional hydrogen bonding is most essential interaction that lead to the association of peptidic units into one-dimensional (1D) objects among other types of entropic and enthalpic contributions, like hydrophobic forces, electrostatic interactions, and π - π interactions. Because of the

supramolecular nature, changes in temperature, pH, ionic strength or the presence of other molecules can successfully trigger the formation of supramolecular hydrogels (Fig. 1B). Peptide-based hydrogels have receiving rapidly growing interest recently due to their obvious merits---inherent biodegradability, biocompatibility and the ability to interact with biology. Peptides with a small molecular weight can be easily synthesized using solid-phase peptide synthesis techniques and purified with high-performance liquid chromatography (HPLC). Due to the chemical and structural diversity of amino acids allowing a great variety of design parameters, the mechanical, physicochemical, and biological properties of the resulting gels can be easily tuned. Peptide based hydrogel systems can be divided by four major classes: unconjugated small molecule native peptides [39-40], peptide amphiphiles [41-43], aromatic peptides [34,44,45] and drug amphiphiles [46-53]. In this thesis, I focus on the supramolecular hydrogels formed by drug amphiphiles.

Cui and co-workers designed a type of self-assembling peptide drug conjugates in a way to functionally mimic protein-drug conjugates [54]. These conjugates are formed by anticancer drugs and a rationally designed peptide which, due to the biological function and assembly potential of short peptides, are able to self-assemble into high-aspect-ratio filamentous structures in aqueous solution, further forming self-supporting hydrogels. In addition, alternating the conjugated drug or optimizing biologically active peptide sequences results in easy tuning of the overall property/functionality of these filaments, providing a novel platform for effective cancer treatment.

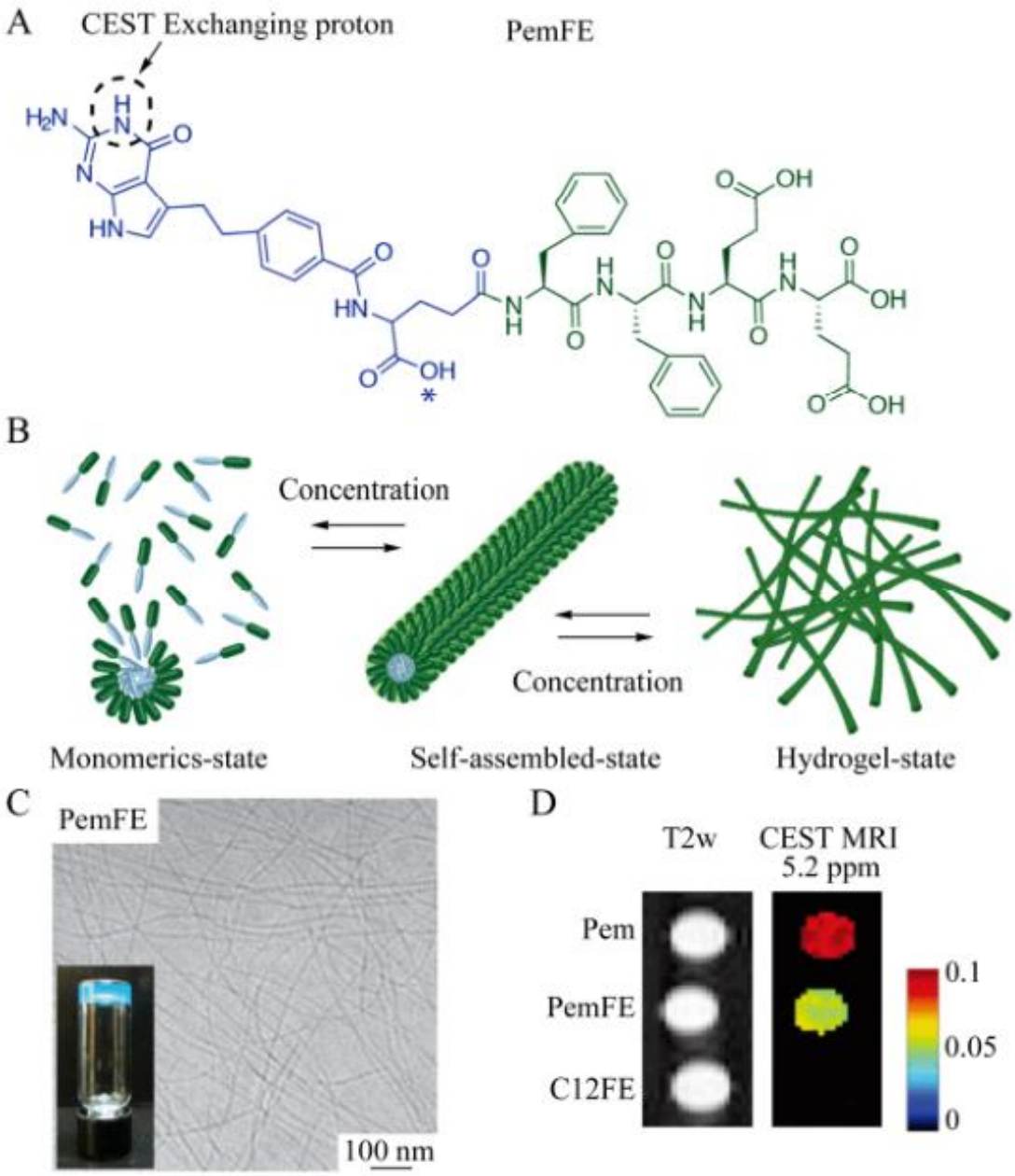

Fig.2 The design of one-component theranostic hydrogels: (A) Design and chemical structure of Pem-FFEE DA; (B) Cartoon illustration of self-assembly of DAs into nanofibers and entanglement of fibers into hydrogels;(C) Cryo-TEM image of fibers formed by Pem-FFEE and optical picture of Pem-FFEE hydrogel; (D) In vitro CEST imaging of Pem-FFEE hydrogels with free Pem and C12-FE as controls (Reprinted with permission from Ref. [46]; Copyright (2017) American Chemical Society)

Lock *et al*. recently reported a supramolecular strategy to conjugate an anticancer drug, Pemetrexed(Pem), to a supramolecular hydrogelator with inherent chemical exchange saturation transfer(CEST) MRI signals [46]. A Pem molecule was conjugated onto a short peptide sequence containing two glutamic acids and two

phenylalanines. In their design, Pem consisting aromatic amines and secondary amines in its chemical structure, serving as both an anticancer drug and a noninvasive MRI contrast agent. The two hydrophilic negative charged glutamic acids were incorporating to increase the water solubility of hydrophobic Pem drug. The π - π interactions from two aromatic phenylalanines promote the self-assembly of the resulting drug amphiphiles. This rationally designed PemFE drug amphiphiles are capable of associating into filamentous nanostructures and further entangle into a 3D network to fabricate self-supportive hydrogels(Fig 2B and 2C). They found incorporating of two phenylalanine significantly improving the potential of prodrug molecules to form supramolecular filamentous structures and hydrogels. They also found the location, distribution, recovery, and drug release of the injected PemFE drug amphiphiles can be detected by CEST MRI in a mouse glioma model. In this study, a highly novel strategy to develop metal-free, MRI-guided theranostic supramolecular hydrogel delivery platform as a safer way for imaging-guided cancer therapy was shown.

1.2 Supramolecular nanostructures formed by drug amphiphiles

The effective treatment of both primary and secondary (metastatic) cancers requires the systemic delivery of drugsto ensure exposure of all cancer sites to the anticancer agents. Molecular hydrogels have many merits for local delivery and treatment of the primary tumor but cannot efficiently affect any metastatic tumors that may have formed prior to treatment. A nanostructure-based strategy to this issue is the covalent modification of drugs in such a way as to form discrete nanostructures that can remain soluble without further aggregation of nanostructures. These PDCs, termed drug amphiphiles (DAs), are formed by covalently conjugating one or more anticancer drugs to a rationally designed/chosen peptide through a biodegradable linker [7-12].

Cui et al, reported the supramolecular strategy enabling the direct assembly of CPT DAs into discrete, stable and well-defined nanostructures with a high and quantitative drug loading [54]. Due to the branching point on the two amine functional amino acid lysine, conjugation of one, two or four CPT molecules can be achieved by attaching cysteine, resulting in fixed drug loadings of 23%,31% and 38% [Fig 3].

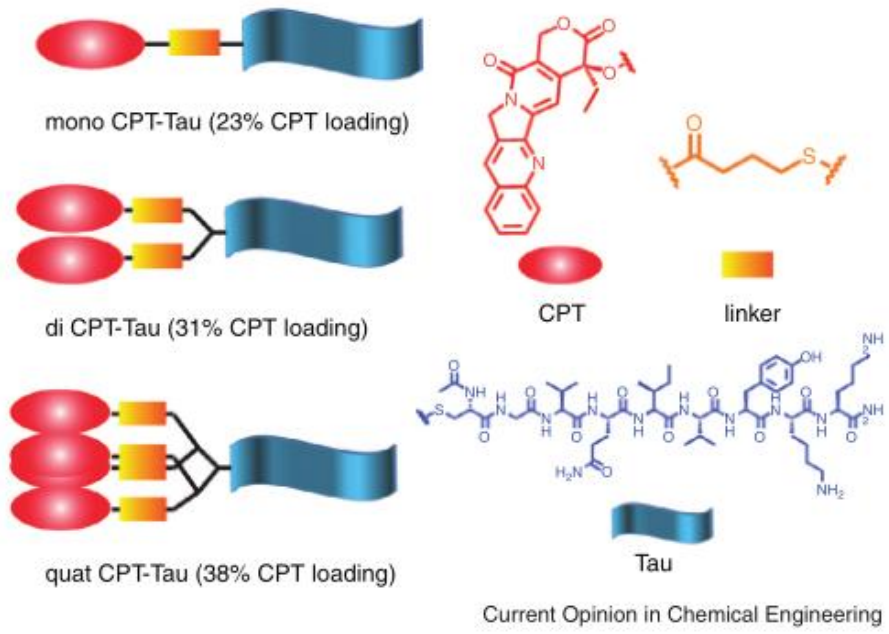

Fig.3 Rational design of self-assembling drug amphiphiles. Self-assembling CPT-Tau conjugates with different CPT units. These drug amphiphiles do not have any dispersity in molecular weight and can be purified by HPLC (Reprinted with permission from Ref. [54]; Copyright (2013) American Chemical Society)

The morphologies of the nanostructures also changed from nanofibers to nanotubes with the change of drug content. In addition, stability of these nano-sized assemblies formed by these drug amphiphiles is rather strong. Only when the concentration decrease to the nano-molar range by dilution, the dissociation occurred. That may result from the increasing hydrophobicity in combination with possible π–π associative interactions among the CPT units. CPT release can be achieved by adding the cancer-relevant reducing agent GSH.

Su et al. recently reported a supramolecular platform of self-assembling prodrugs (SAPDs) that are able to associate into filamentous nanostructure in aqueous solution [55]. In their molecular design, two CPT molecules were conjugated to three different types of short hydrophilic peptide sequences to generate three SAPDs, including dCPT-K_2 , dCPT-OEG5 -K_2 and dCPT-Sup35-K_2 ,which all are capable of self-assembling into high-aspect-ratio one-dimensional nanostructures. However the internal molecular packing of the prodrug building units is different. dCPT-K_2 and dCPT-OEG_5 -K_2 associated into nanotubes with a hollow center because they do not possess a β -sheet-forming peptide sequence, while dCPT-Sup35-K_2 with the β -sheet-forming peptide sequence in the middle assembled into core-shell nanofibers. Strong π - π interactions between CPT units dominate the formation of nanotubes and the lack of the strong, ordered intermolecular hydrogen bonding from Sup35 moieties afforded for a higher degree of packing between the CPT units into tubular structures. The incorporation of a β -sheet-forming peptide sequence may result in the formation of the nanotubes because the β-sheet-forming peptide sequence demonstrates the arrangement of intermolecular hydrogen bonding. They also found that nanotubes were much more stable than nanofibers. Additionally, they found these SAPDs possess a comparable efficacy against primary brain cancer cells over the free CPT. Their findings support that π - π interactions could influence the formation of one-dimensional filaments. Due to this platform technology of self-assembling high potent long filaments, rational design of supramolecular prodrug-based hydrogels for local cancer chemotherapy can rapidly be developed.

Ma et al. recently showed a follow-up reports about a self-assembling hybrid prodrug system containing both a CPT and a capecitabine (Cap) analogue (Fig.4) [56]. They found that assembled morphology of prodrugs and nanostructure stability

can be strongly influenced by the chemical structure of anticancer drug. The nanostructures varied from long core-shell nanofibers to long filaments then to spherical particles with decreasing the number of CPT molecules. They also found that CPT-Cap filaments exhibited a synergistic effect and obviously improved potency against three esophageal adenocarcinoma cell lines over two homo-prodrugs and free parent drugs.

This example demonstrated integration of two structurally distinct drugs into a single self-assembling hybrid prodrug that provides strategy of fabricated self-deliverable, one-dimensional filaments as excellent candidates fir hydrogel.

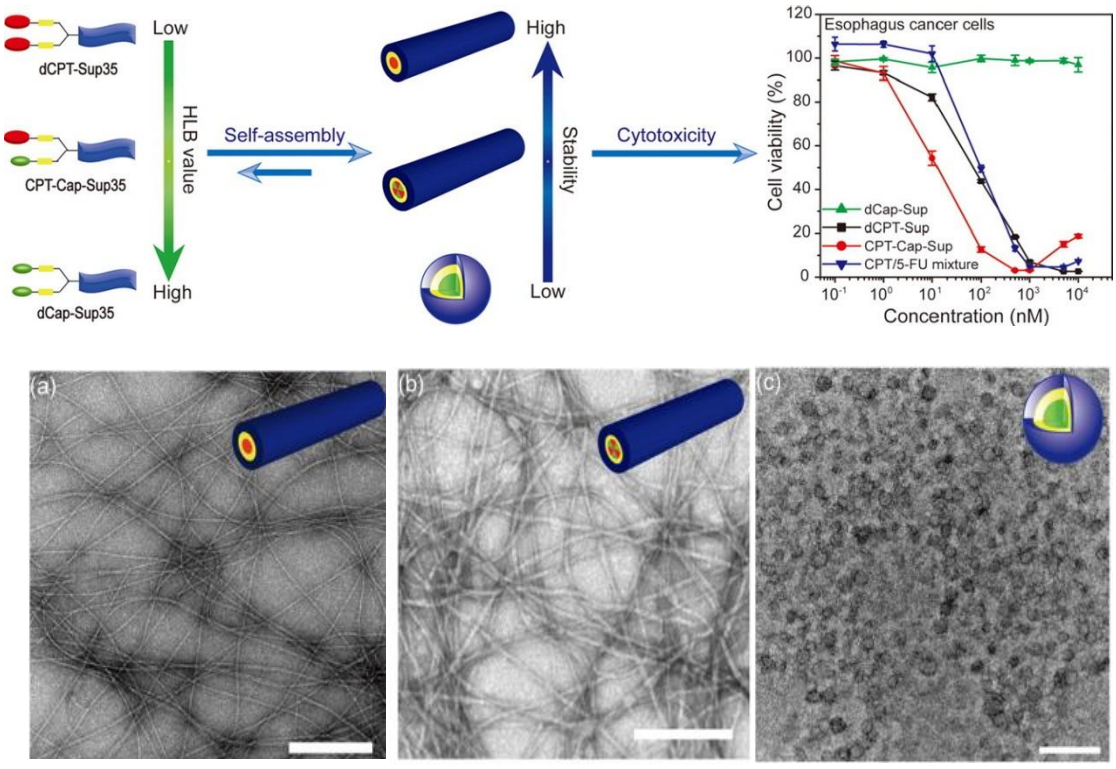

Fig. 4 Chemical structure of dCPT-Sup35, CPT-Cap-Sup35 and dCap-Sup35 and illustration of their corresponding assembled nanostructures and TEM images of three different drug amphiphiles. (Reprinted with permission from Ref. [56]; Copyright (2017) Elsevier)

1.3 Stability of self-assembling drug amphiphiles in biologic environments

The surface of nanosized materials possess higher free energy than the bulk material itself, indicating that surface of nanoparticles will progressively and selectively absorb biomolecules when they contact with complex biological fluids [58-61]. Adsorption of proteins form physiological fluids to nanocarriers results in the formation of a protein shell. This rapidly forming protein corona is responsible for the biological fate of nanocarriers [62-65]. Poly-(ethylene glycol) is widely used to reduce any non-specific protein adsorption and PEGylated drugs and nanovehicles exhibit longer blood half-lives and less non-specific cellular uptake. For surfaces, PEGlation is also used to reduce protein adsorption [66-70]. This feature is always called “stealthy effect”, which can be explained by the high level of hydration of the hydrophilic polyether, preventing protein adsorption on typically hydrophobic polymer surfaces by steric repulsion [71-74]. So in this thesis , we want to study weather OEG, the monomer of PEG, can reduce protein adsorption of self-assembling nanostructures and subsequently incress the nanostructure stability in biological environments compared with other drug amphiphiles with different surface charge.

2. Materials and Methods

2.1 Synthesis and molecular characterization

2.1.1 Materials

Fmoc amino acids (except Fmoc-Lys(Fmoc)-OH) and coupling reagents (HBTU) were purchased from Advanced Automated Peptide Protein Technologies (AAPPTEC, Louisville, KY, USA). Rink aminde MBHA resin and Fmoc-Lys(Fmoc)-OH were purchased from Novabiochem(San Diego, CA, USA). Camptothecin was obtained from AvaChem Scientific (San Antonio, TX, USA) and all other reagents were purchased from Sigma-Aldrich (St. Louis, MO) or VWR (Radnor, PA, USA).

RP-HPLC was performed on a Varian Prostar Model 325 HPLC (Agilent Technologies, Santa Clara, CA, USA) with a fraction collector. Preparative separations were performed using a Varian PLRP-S column (100 Å, 10 μm, 150 mm×25 mm), while analytical HPLC utilized a Varian Pursuit CRs C18 column (5 μm, 150 mm×4.6 mm). The mobile phase was acidic solutions (water and acetonitrile containing 0.1% v/v TFA). Purified target molecules were lyophilized using a FreeZone -105℃ 4.5L freeze dryer (Labconca, Kansas City, MO). ESI-MS mass spectrometric data for characterization was obtained using a Finnigan LDQ Deca ion-trap mass spectrometer (Thermo-Finnigan, San Jose, CA).

2.1.2 Peptide Synthesis

All peptide conjugates, $(Ac\text{-}Cys)_2KK_2$ ($dCys\text{-}K_2$), $(Ac\text{-}Cys)_2KE_2$ ($dCys\text{-}E_2$), $(Ac\text{-}Cys)_2K(OEG_5)_2$ ($dCys\text{-}(OEG_5)_2$), $(Ac\text{-}Cys)_2KKE$ (dCys-KE) and

$(Ac\text{-}Cys)_2KEK$ (dCys-EK), here were manually synthesized on the Rink Amide MBHA resins with the scale of 0.25 mmole by utilizing standard 9-fluorenylmethoxycarbonyl (Fmoc) solid phase synthesis techniques. Fmoc deprotections were performed using 20% 4-methylpiperidine in DMF solution for 15 minutes, repeating once. The amino acid coupling cycle was followed by adding a mixture of Fmoc-amino acids, HBTU and DIEA at a ratio of 4:4:6 relative to resin in DMF for 2 h. The conjugation of Fmoc-NH-OEG_5-Propionic was performed using the same protocols as amino acids coupling. The branching point was realized by adding Fmoc-Lys(Fmoc)-OH to generate two amino groups before the coupling of Fmoc-Cys(Trt)-OH. Acetylation was performed at N-terminus of amino acids utilizing a 20% acetic anhydride in DMF solution with 100 μL DIEA for 15 min, repeated twice. In all cases, reactions were monitored by the ninhydrin test (Anaspec Inc., Fremont, CA) for free amines. All completed peptides were cleaved from the Rink resins using standard cleavage solution of TFA/TIS/H_2O (92.5:5:2.5) for 3 h. Excess TFA was removed by air blow and the remaining peptide solution was precipitated in cold diethyl ether to obtain crude products, which were phase-separated from diethyl ether using centrifugation technique (5900 rpm for 4 min) and dried under vacuum overnight.

2.1.3 Peptide Purification

Peptide purification was achieved on RP-HPLC using a Varian ProStar model 325 HPLC (Agilent Technologies, Santa Clara, CA, USA) equipped with a fraction collector. All crude peptides were dissolved in 20 mL of 0.1% v/v TFA and

purification run was carried out with a 10 mL injection. A water/acetonitrile gradient 10%-90% was ran for 30 minutes containing 0.1% v/v TFA at a flow rate of 20 mL/min. The 220 nm signal from UV-Vis detector was used to trigger the fraction collector for preparative RP-HPLC. Collected fractions were identified by ESI-MS (LDQ Deca ion-trap mass spectrometer, Thermo Finnigan, San Jose, CA) and the ones containing desired products were lyophilized (FreeZone -150 ℃ 4.5L freeze dryer, Labconco, Kansas City, MO) and stored in -30℃ fridge.

2.1.4 Electrospray Ionization-Mass Spectra (ESI-MS)

ESI mass spectra were acquired on a Finnigan LDQ Deca ion-trap mass spectrometer equipped with an electrospray ionization source (Thermo Finnigan, San Jose, CA). Samples were in DI water with 5% of acetonitrile containing 0.1% v/v NH_4OH and introduced into the instrument at a rate of 10 □L/min using a syringe pump via a silica capillary line. The heated capillary temperature was 250 ℃ and the spray voltage was 5 kV.

2.1.5 Analytical HPLC Characterization

Analytical RP-HPLC was performed using a Varian polymeric column (PLRP-S, 100 Å, 10 μm, 150 mm× 4.6 mm) with 20 μL injection volume. A water/acetonitrile gradient 15%-85% was run for 20 minutes containing 0.1% v/v TFA at a flow rate of 1 mL/min.

2.1.6 Drug Amphiphile Synthesis and Characterization

The synthesis of drug amphiphiles was achieved by mixing CPT-etcSS-Pyr and the corresponding crude peptides in 2 mL of N_2-purged DMSO with a molar ratio

of 2:1 and allowing them to react for 5 days. The mixture was diluted to 10 mL in acetonitrile/water with 0.1% v/v TFA and purified by preparative RP-HPLC using a Varian ProStar model 325 HPLC (Agilent Technologies, Santa Clara, CA, USA) equipped with a fraction collector. Separations were carried out on a Varian PLRP-S column (100 Å, 10 μm, 150 mm×25 mm) monitoring at 370 nm. Collected fractions were probed by ESI-MS (LDQ Deca ion-trap mass spectrometer, Thermo Finnigan, USA), and the fractions with targeting molecules were collected, concentrated and lyophilized on a FreeZone -105 ℃ 4.5 L freeze dryer (Labconco, Kansas City, MO, USA). The powders obtained were then re-dissolved, calibrated and aliquoted into cyro-vials before re-lyophilization.

2.1.7 Concentration calibration

The concentrations of purified drug amphiphiles were calibrated by analyzing the reduced product free CPT from drug amphiphiles. Briefly, all samples were dissolved in MeCN/H_2O (1:1) to obtain the stock solutions. 5 μL of the stock solution was then diluted to 20 μL by addition of 15 μL MeCN/H_2O (1:1) and mixed with 20 μL of 1 M aqueous TCEP for 1 h by periodic vortexing to allow disulfide bond cleavage and obtain free CPT from drug amphiphiles. To measure the area of the peak resulting from free CPT at 370 nm, 30 μL of solution was then injected into the HPLC. The concentration of CPT was obtained by comparing the area of the peak from TCEP-treated solution with the standard calibration of CPT. The drug amphiphile concentration was further calculated by the applied dilutions and the number of CPT molecules. The stock solution was diluted to 400 μM according to the

calibrated concentration and aliquoted into cyro-vials before re-lyophilization.

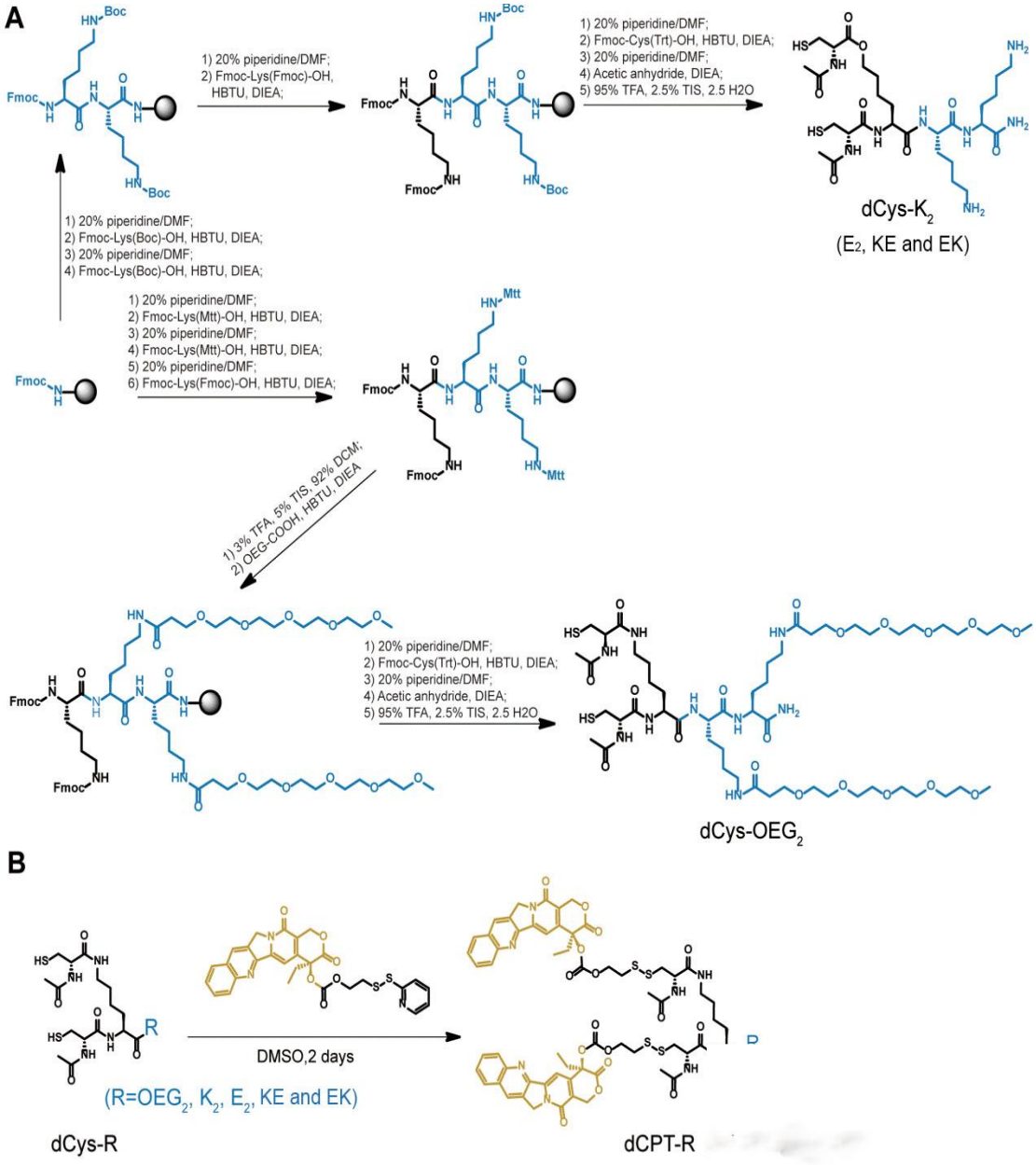

Fig. 5 Schematic illustration for synthesis of drug amphiphiles. (A) Synthetic routes of peptide segments dCys-K_2 and dCys-OEG_2 using standard Fmoc solid phase peptide techniques (dCys-E_2, dCys-KE and dCys-EK use the similar protocols as dCys-K_2). (B) Synthesis of functional drug amphiphiles by mixing peptide segments synthesized in (A) with CPT-etcSS-Pyr in DMSO.

2.2 Self-assembly characterization

2.2.1 Transmission electron microscopy (TEM) imaging

200 μM solutions of corresponding samples in 1×DPBS were prepared by directly dissolving respective lyophilized powders, and allowed to age overnight. TEM samples were prepared by depositing 10 μL of the respective solution onto a carbon-coated copper grid (Electron Microscopy Services, Hatfield, PA, USA), wicking away the excess solution with a small piece of filter paper. 10 μL of a 2 wt% uranyl acetate aqueous solution was then deposited on the surface and after 30 seconds the excess solution was removed as above to leave a very thin layer. The sample grid was then air-dried at room temperature at least 3 hours prior to imaging. Bright-field TEM imaging was performed at an acceleration voltage of 100 kV on the Tecnai 12 TWIN transmission electron microscopy instrument equipped with 16 bit 2K×2K FEI Eagle bottom mount camera (FEI, Hillsboro, OR) and SIS Megaview III wide-angle CCD camera.

2.2.2 Cryogenic TEM imaging

Cryo-TEM imaging was performed at a higher concentration of 800 μM compared with 200 μM in conventional TEM imaging, since higher concentration allows more rapid visualization of the structures and reduces possibility of damage to vitreous ice film caused by the electron beam during imaging. 6 μL of the appropriate solution was dropped onto a lacey carbon film supported TEM copper grid (Electron Microscopy Services, Hatfield, PA, USA). All the TEM grids used for cryo-TEM imaging were treated with plasma air to render the lacey carbon film hydrophilic. A

thin film of the sample solution was produced using the Vitrobot with a controlled humidity chamber (FEI). After loading of the sample solution, the lacey carbon grid was blotted using preset parameters and plunged instantly into a liquid ethane reservoir precooled by liquid nitrogen. The vitrified samples were then transferred to a cryo-holder and cryo-transfer stage that was cooled by liquid nitrogen. To prevent sublimation of vitreous water, the cryo-holder temperature was maintained below -170°C during the imaging process. All images were recorded by a 16 bit 2K × 2K FEI Eagle bottom mount camera.

2.2.3 Circular dichroism

CD spectra were recorded on a Jasco J-710 spectropolarimeter (JASCO, Easton, MD) from 190 nm to 480 nm using a 1 mm (for 100 μM and 50 μM) or 10 mm (for 12.5 μM and 3.125 μM) path length quartz UV-Vis absorption cell (Thermo Fisher Scientific, Pittsburgh, PA, USA). Background spectra of the solvents were obtained and subtracted from the sample spectra. The mean residue ellipticity [θ] was calculated by the following equation

$$[\theta] = \frac{\theta}{lCn}$$

Where θ is the acquired ellipticity in deg, C is the concentration of the drug amphiphiles calibrated by analyzing the reduced product free CPT, l is the light path length of the quarts UV-Vis absorption cell, and n is the number of amino acid residues.

2.2.4 Determination of critical micellization concentration (CMC)

The determination of CMC values were performed according to the modified

protocol of a reported work. Identical volume of the Nile Red solution which was initially prepared by dissolving the dye in acetone was loaded in centrifuge tubes. Dry mass of Nile Red was yielded by solvent evaporation under room temperature. Various concentrations of the drug amphiphile solution were prepared in H2O or PBS, and then added into the centrifuge tubes with same amount of Nile Red solids. These mixtures of Nile Red and drug amphiphiles after vortexing were incubated in the dark at room temperature overnight to assume equilibrium. Fluorescent spectra of Nile Red were detected by a Fluorolog fluorometer (Jobin Yvon, Edison, NJ) with fixed excitation wavelength at 560 nm; emission spectra were monitored within 580-720 nm. The ratios of the emission intensity at 635nm (near the emission maximum when Nile Red was encapsulated in the hydrophobic environments) to that at 660 nm (the weak emission maximum in aqueous conditions) were then plotted against the drug amphiphiles concentrations. The surge in intensity ration (I635/I660) reveals the dye being encapsulated into the hydrophobic environments in assembled structures because the Nile Red was strongly quenched in aqueous conditions, while this transition occurs as the incubated drug amphiphiles exceed their CMC values. The CMC values were obtained by calculating the crossover point of the ratio curve plotted against the drug amphiphile concentrations before/after the intensity surge.

2.2.5 Physical stability of five different charged nanotubes

We next investigated the stability of five different charged nanotubes upon dilution in cell medium using CD spectrometer. To get rid of the influence of phenol red in spectrometer, we used DMEM (phenol red free, Mediatech) containing 10%

fetal bovine serum (FBS, Invitrogen) and 1% antibiotics (Invitrogen) as cell medium solution. The stock solutions of these molecules were prepared at the concentration of 1 mM in water and aged overnight. The aged solution was diluted to 200 μM with cell medium. After that, solutions containing 200 μM of these nanotubes in cell medium were further diluted to 100 μM, 50 μM, 25 μM, 10 μM and 5μM. All the diluted solutions were incubated for another two days before CD measurement. All the CD spectra were recorded from 300 to 480 nm using a 1 mm (for 200 μM, 100 μM and 50 μM) or 10 mm (for 25 μM, 10 μM and 5 μM) path length quartz cell. The spectra were collected and normalized from ellipticity (mdeg) to molar ellipticity (deg· cm2 ·dmol−1). No significant changes were observed from the normalized curves, indicating no obvious disassociation of the self-assembled nanotubular structures at the concentration above 5 μM. In addition, the solution of nanotube in cell medium remained clear after one week, suggesting no obvious aggregation of nanotubes in cell medium.

2.2.6 UV-Visible spectroscopy

The solutions of these different drug amphiphiles in DMEM with 10% FBS and human serum at concentration 200 μM were measured using a UV-Visible double beam spectrophotometer (UV-1601 PC, Shimadzu, Japan; H14 grating UV) through optical resolution of 0.4 nm. Transparent degree measurements of these solution were obtained over wavelength of 200-600 nm at room temperature using quartz cuvettes (1 mm path length). We carried out transparent degree measurements of the same solutions during two weeks at different time point to study the stability of these drug

amphiphiles in DMEM with 10% FBS or human serum. The cuvettes were cleaned before each use by sonicating for 5 min in deionized water followed by rinsing with deionized water.

3. Results and Discussion

3.1 Synthesis of self-assembling different charged drug amphiphiles

The synthesis was realized in a modular and efficient fashion utilizing established synthetic strategies. Briefly, the different charged peptide segments with two N-terminal cysteine residues (dCys-K_2, dCys-E_2 , dCys-OEG_2, dCys-KE, dCys-EK) were first synthesized using standard Fmoc solid-phase synthesis protocols. To conjugate CPTs onto the peptide, the disulfide formation reaction was then performed in nitrogen-purged DMSO as reported previously. The molecular masses of the final products were confirmed using electrospray ionization mass spectroscopy, and their purity was confirmed using analytical HPLC.

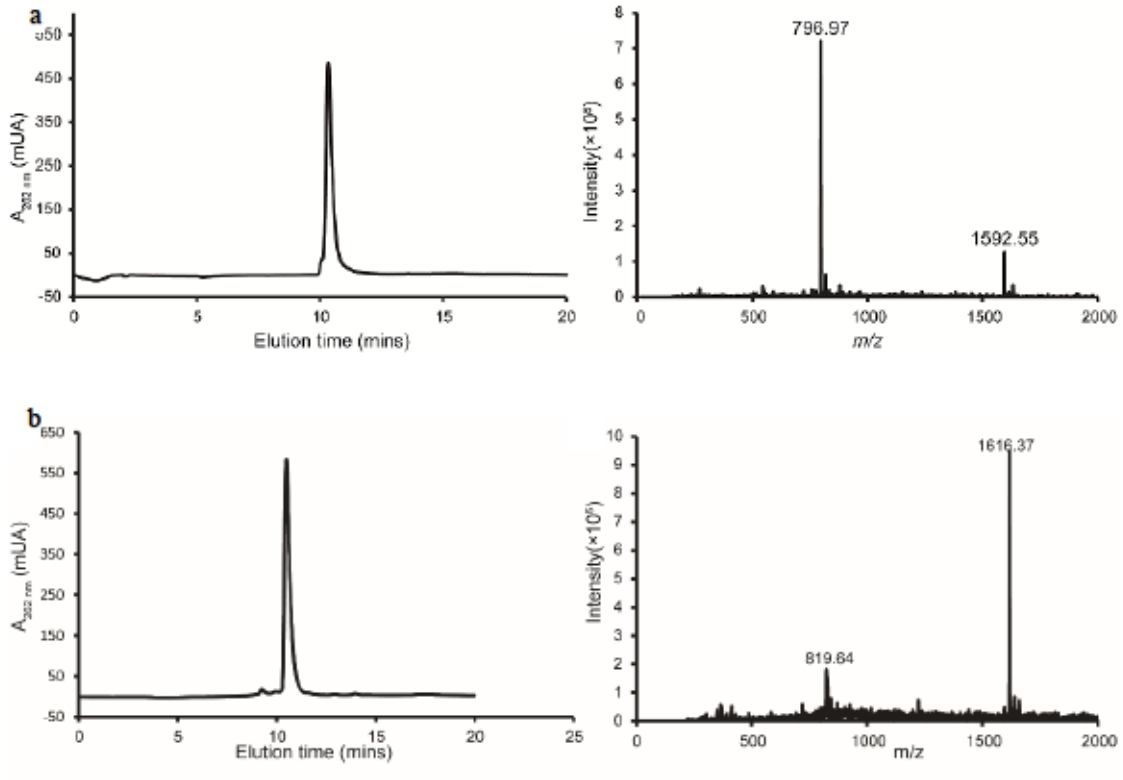

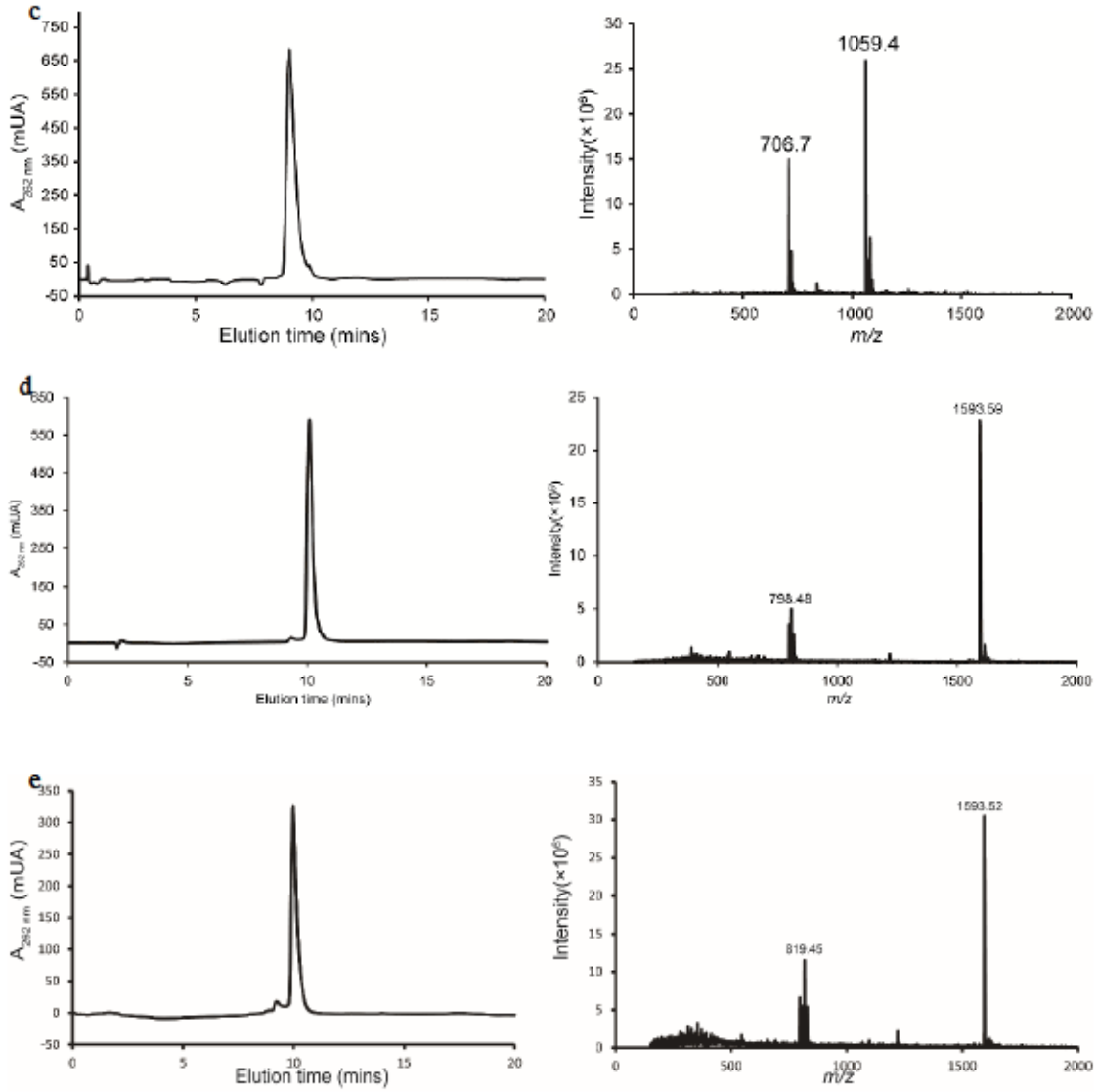

Fig. 6 RP-HPLC and ESI-MS spectrum of dCPT-K_2 (a). The peaks at 796.97 and 1592.55 correspond to $[M+H]^{2+}$ and $[M+H]^{+}$, respectively. RP-HPLC and ESI-MS spectrum of dCPT-E_2 (b). The peaks at 819.64and1616.37 correspond to $[M+Na]^{2+}$ and $[M+Na]^{+}$, respectively. RP-HPLC and ESI-MS spectrum of dCPT-OEG_2 (c). The peaks at 706.7 and 1059.4 correspond to $[M+2H]^{2+}$ and $[M+H]^{3+}$, respectively. RP-HPLC and ESI-MS spectrum of dCPT-KE (d). The peaks at 798.48 and 1593.59 correspond to $[M+2H]^{2+}$ and $[M+H]^{+}$, respectively. RP-HPLC and ESI-MS spectrum of dCPT-EK (e). The peaks at 819.45 and 1593.52 correspond to $[M+Na]^{2+}$ and $[M+H]^{+}$, respectively.

3.2 Self-assembly of drug amphiphiles

The self-assembling molecules containing a bent-shaped aromatic segment with an internal angle of 120° tend to associate into tubular nanostructures. In this

project, we conjugated crescent-shaped anticancer drug, camptothecin (CPT) to hydrophilic peptide sequences to generate self-assembling prodrugs. The self-assembly of cationic prodrug, dCPT-K_2, was initiated by dissolving the lyophilized molecules into deionized water. The regular TEM image showed that dCPT-K_2 self-assembled into hollowed soft nanotubes in DI water at concentration 200 μM, after aged for 1 day at room temperature. According to the diameter analysis of dCPT-K2 nanotubes obtained from the TEM image, their diameters are 8.3 nm. In addition, the lengths of these nanotubes are in micrometer range. Circular dichroism spectrum of dCPT-K2 at 200 μM in aqueous solution (Figure) indicated the ordered chiral pack of internal aromatic CPT moieties. Two bisignate CD signals at 266 nm and 367 nm are due to strong exciton coupling between neighboring CPT aromatic rings. The strong positive signal centered at 389 nm is resulted from a positive chirality and a right-handed helical arrangement of the planate CPT units. The one-dimensionality of the nanotubes is further confirmed by the negative β-sheet signal at around 223 nm for peptide region. All these results reveal that cationic prodrug self-assembles into nanotubes with a monolayered pattern and strong π-π interaction resulting from bent-shaped CPT units is essential for tubular structure of the molecule.

Assembled morphologies are able to be switched by altering the hydrophilic segments which leads to the changes in the crucial hydrophilic-lipophilic balance, electrostatic interactions and hydrogen bonding. Only when one of the interactions so strong to dominate the whole self-assembling process can same nanostructures be built with different self-assembling monomers. In this project, we envision that due to the strong packing of hydrophobic CPT moieties, the self-assembling tubular morphologies of prodrugs will not be significantly changed by other small molecule functional hydrophilic segments. Conventional TEM images reflected

the one-dimensionality of those nanotubes with the emblematic dark centerlines. The length of these assembled aggregates are all up to micrometer scales and the diameters are in the range of 8.5-10.5 nm. Thus, anionic, zwitterionic, non-ionic prodrugs can also self-assemble into nanotubes at the same condition with cationic prodrug. In order to confirm the formation of the nanotubes, we further carried out the circular dichroism (CD) measurements of all these prodrugs at 200 μM. A strong negative signal at around 223 nm was observed in five molecules, revealing the formation of β-sheet secondary structure of peptide segment in the self-assembled state, which consists with the one-dimensionality of the nanotubes. Also the CD spectra show two bisignate CD centered at 266 and 367 nm due to strong exciton coupling between adjacent CPT aromatic rings, and a strong positive signal at 389 nm resulting from a positive chirality and a right-handed helical arrangement of the planar CPTs. All these CD spectra reveal the packing of all assembled aggregates are in a similar fashion. Closer or looser packings of the building units influenced by the total amphiphilicity, electrostatic interaction as well as hydrogen bonding caused the CD intensity differences among those prodrugs.

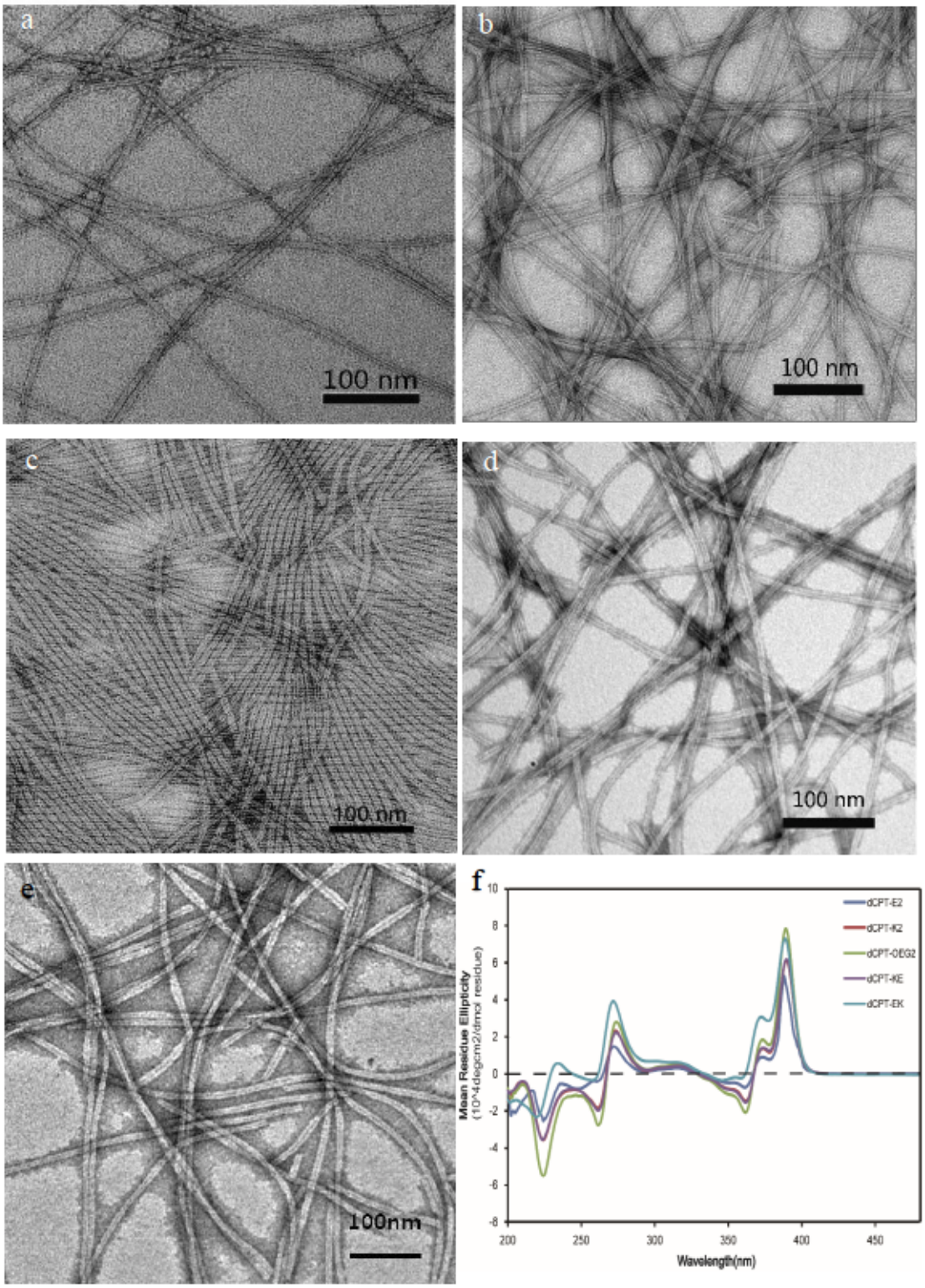

Fig. 7 TEM images of dCPT-K_2 (a), dCPT-E_2(b),DCPT-OEG_2 (c),dCPT-KE (d) and dCPT-EK(e) at a concentration of 200 uM in PBS and CD spectrum of these drug amphiphiles(f)

Critical micellization concentrations (CMC) of these drug amphiphiles with different charge in 1X PBS were first determined using Nile red as a probe, which

intensely fluoresces in hydrophobic core of nanostructure but is highly quenched and red-shifted in aqueous solution. Plotting the ratio of intensity at 635 nm (emission maximum of the encapsulated dye) to that at 660 nm (emission maximum in aqueous conditions) against the concentration of each drug amphiphile indicates the transition that occurred when the molecule concentration surpass the CMC. No obvious difference was observed in calculated CMC values, within a range of 2-5 μM, of these different charged drug amphiphiles, indicating that surface charges of these assemblies have a minor impact on associating concentration values which are mainly due to the strong interaction of CPT moieties on the drug amphiphiles.

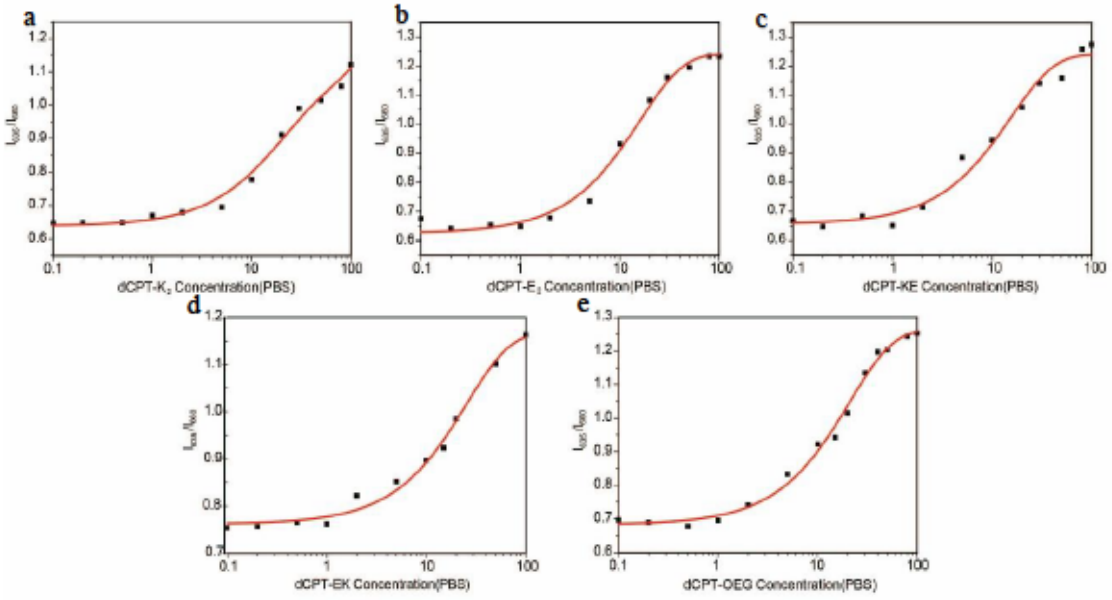

Fig. 8 Calculated CMC values of dCPT-K_2 (a), dCPT-E_2(b), dCPT-OEG_2 (c),dCPT-KE (d) and dCPT-EK(e) in PBS.

We also determined the critical micellization concentrations (CMC) of the nanotubular assemblies in DMEM, a standard cell culture medium, using same encapsulated-dye method. The CMC of the studied peptides was determined by incubating these molecules at various concentrations with a fixed content of Nile red. After plotting the ratio of intensity at 635 nm to that at 660 nm, we found the transition

due to the reason that peptide concentration exceeded CMC (Fig. 8). These drug amphiphiles self-assembling in DMEM possess similar CMC range as them in PBS (Fig. 9).

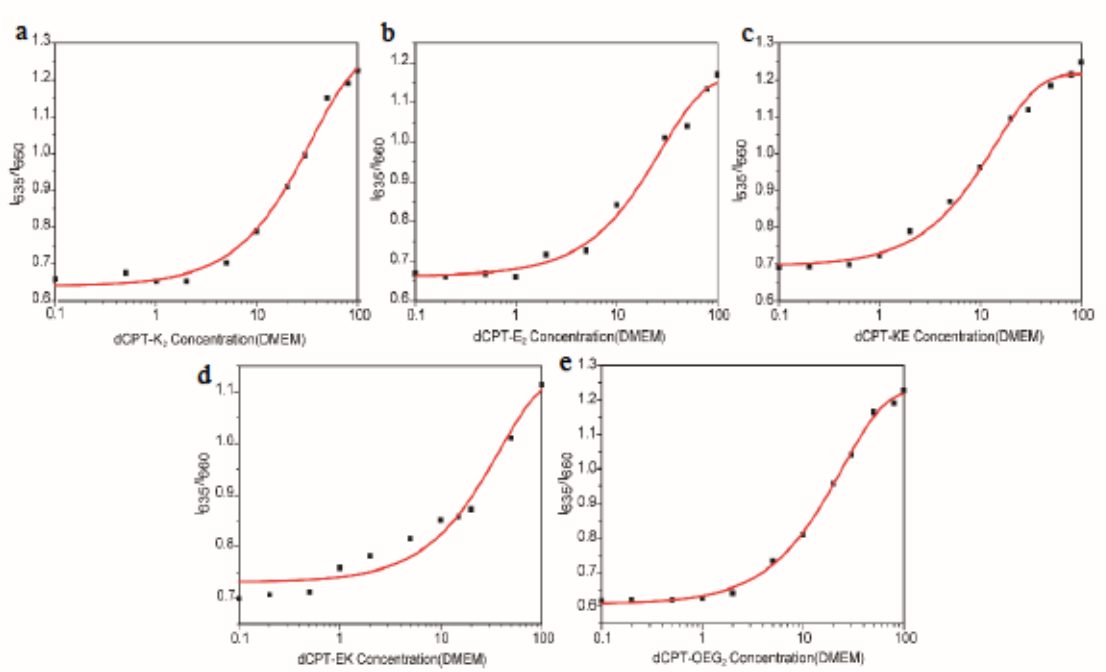

Fig. 9 Calculated CMC values of dCPT-K2 (a), dCPT-E2(b), dCPT-OEG2 (c),dCPT-KE (d) and dCPT-EK(e) in DMEM.

3.3 Stability of self-assembling nanostructures in the presence of proteins

Then we dissolved all drug amphiphiles solutions into DMEM with 10% FBS. Cationic drug amiphiphile, dCPT-K_2, immediately precipitated out resulting from the surface positive charges which possess a strong tendency to unspecifically bind with proteins in the FBS. The other solutions with a initiate transparent status were placed in room temperature over 2 weeks. Except non-ionic drug amphiphiles keep clear after two weeks, the other molecules, including ionic and zwitter-ionic drug amphiphiles showed a different degree of precipitation. Non-ionic nanostructures with OEG protected possess a reduced unspecific protein binding and showed a stronger stability among other drug amphiphile DMEM/FBS solutions.

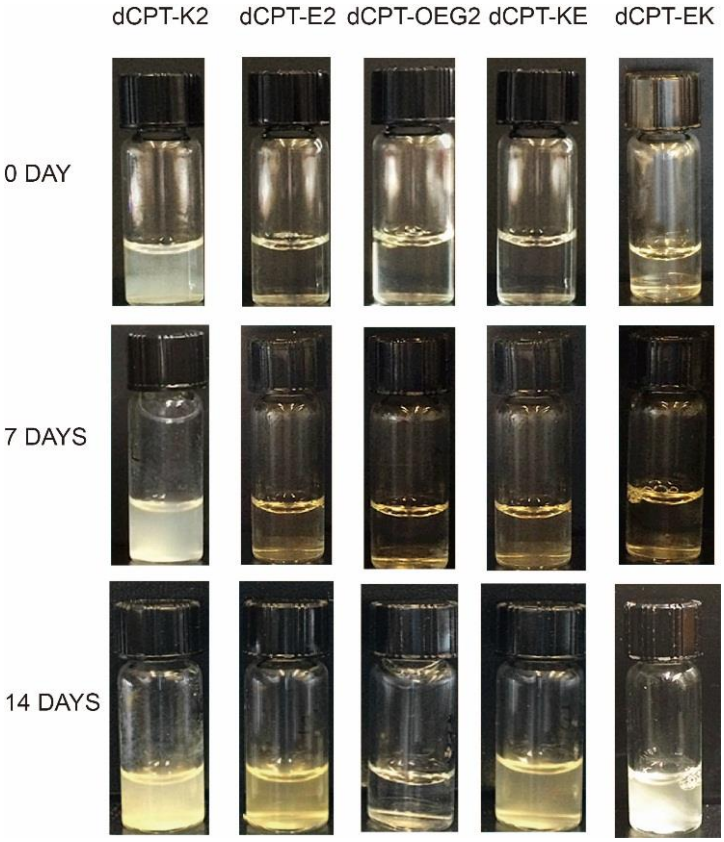

Fig. 10 Photos show the turbidity changes of drug amphiphiles with different surface charges over two weeks. Non-ionic molecules, dCPT-OEG_2, remain clear even after two weeks.

Transmission spectra of the molecules were further monitored by UV-VIS (Fig. 11). The results are consistent with the situation showed in photos over time. The transmission percentage of charged DAs significantly decreased in second week, revealing the solution of these molecules obviously became turbid after two weeks. But the clarity of dCPT-OEG_2 remained as high as its original condition.

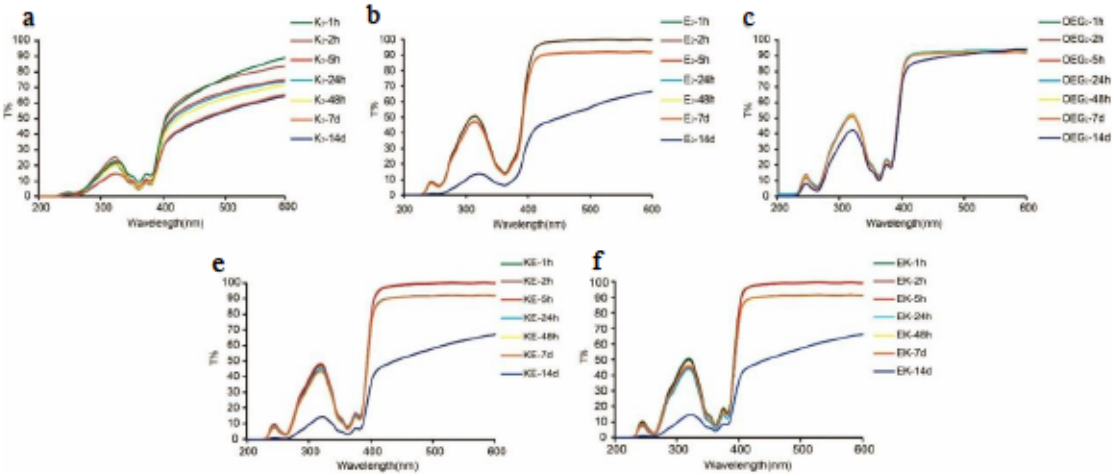

Fig. 11 The transmission spectra detected by UV-Vis showed dCPT-K_2(a), dCPT-E_2(b), dCPT-OEG_2(c), dCPT-KE(d) and dCPT-EK(e) exhibited a different degree of transmission degree change over times

Because of the strong fluorescence of proteins in FBS, the emission spectra of Nile red failed to be detected. Thus CMC values of the drug amphiphiles in the presence of proteins are indirectly speculated by studying the initial concentration of interior CPT packing utilizing CD. The CD spectra of Cationic DA, dCPT-K2 in DMEM with 10% FBS solution were not obtained because of instant dCPT-K2 precipitation in presence of proteins. When the concentration is above 5 um, a positive peak at around 380 nm attributed to the arrangement of CPT in the assembled form becomes obvious, which means CPT molecules of drug amphiphiles started packing with each other at 5 uM, suggesting the aggregation of these DAs occurred when concentration reach 5 uM which is similar with CMC values of these drug amphiphiles without proteins (Fig. 12).

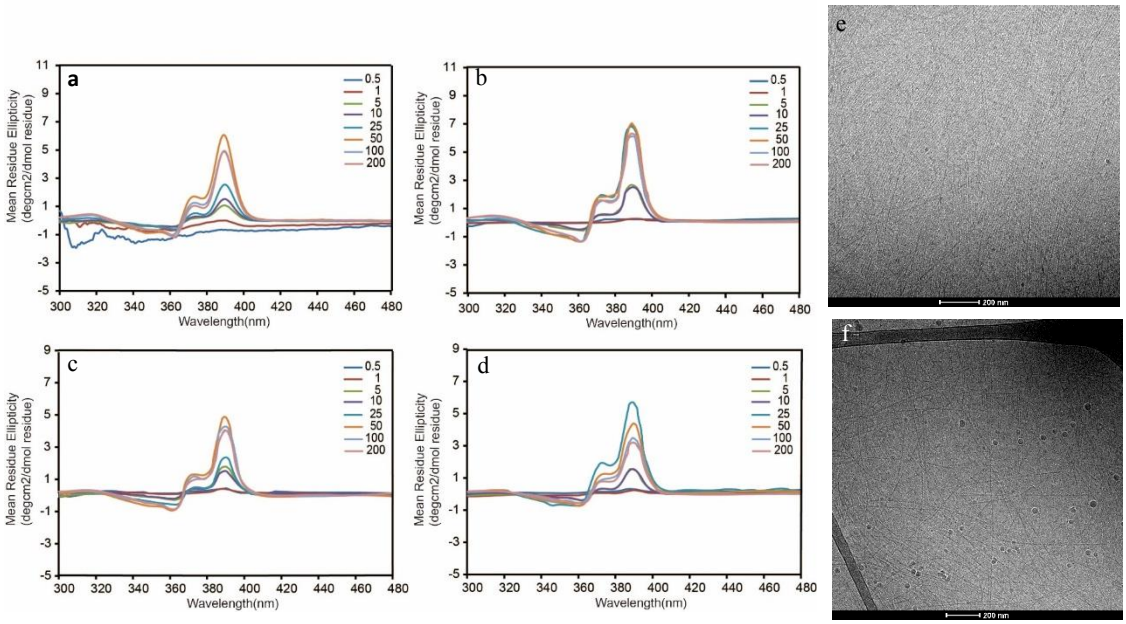

Fig. 12 The CD spectra of dCPT-E2(a), dCPT-OEG2(b), dCPT-KE (c)and dCPT-EK(d) with a wavelength range from 300 nm to 480 nm. Cryo-TEM images of the nanostructures of initial dCPT-OEG2 solution(e) and the solution after one month (f) at a concentration of 200 uM in DMEM with 10% FBS.

According to the cryo-TEM images, the originate solution of non-ionic prodrugs self-assembled into nanotubes which is the same as the nanotubes formed by these prodrugs solution after one month. Because the OEG molecules in self-assembled drug amphiphiles reduce the non-specific protein adsoption, these nanotubes have a better stability (Fig. 12). To better understand the stability of drug amohiphiles , we replaced the FBS with human serum which can better mimic in-situ environments. After dissolving in PBS, these molecules were diluted by human serum. Cationic drug amphiphiles, dDPT-K2, are quickly crushed out, which is the same as dissolving these positive charged molecules in FBS. Then we investigated the turbidity of the other solutions using UV-Vis to monitor the transmission degree (Fig. 13). The results are consistent with the photo of all the solution, showing that non-ionic drug amphiphiles possessed a highest transmission degree. All these results revealed that these molecules with different charges had different interaction with proteins in biological environment.

Cryo-TEM was carried out in order to investigate the nanostructures of drug amphiphiles except cationic one. The differences between the charged nanotubes and the neutral nanotubes were obvious. The nanotubes formed by non-ionic drug amphiphiles are longer, better organized as well as possess a clearer margin than other nanotubes with aggregation of proteins leading to the vague margin of nanotubes. In addition, cryo-TEM images showed the intact and long nonatubes in the initial solution of dCPT-OEG_2 and the solution after one month further demonstrated that nanostructures of self-assembling non-ionic drug amphiphiles can be stable longer in biological environments than other charged drug amphiphiles (Fig. 14).

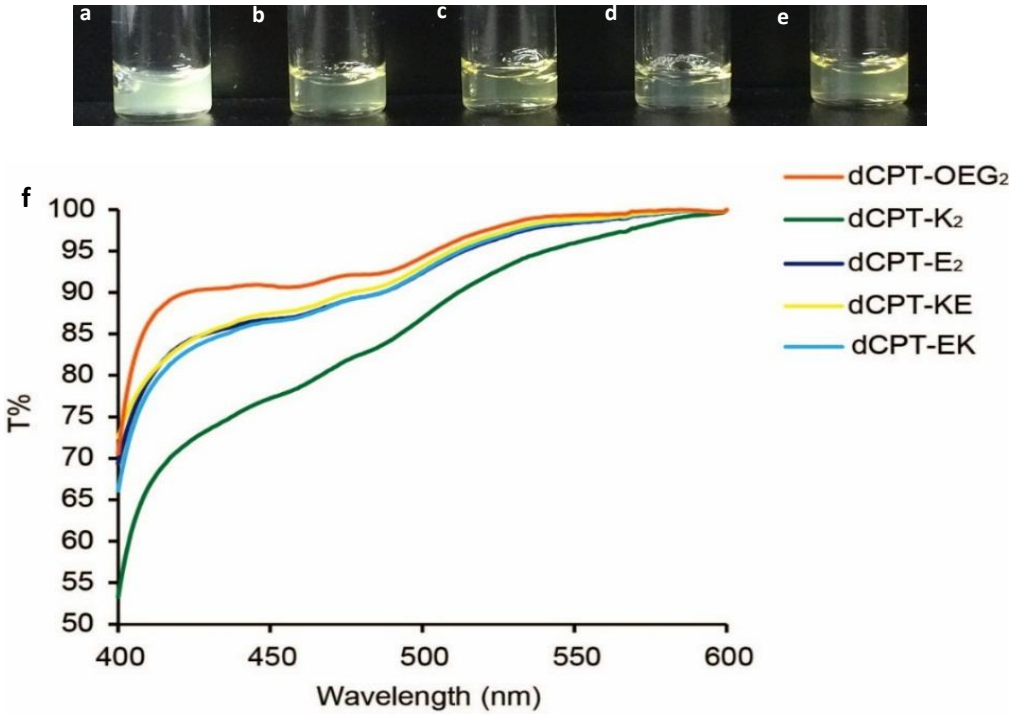

Fig. 13 Photos of the solution of dCPT-K_2(a), dCPT-E_2(b), dCPT-OEG_2(c), dCPT-KE(d) and dCPT-EK(e) in human serum. The transmission spectra of five different charged drug amphiphiles in human serum(f).

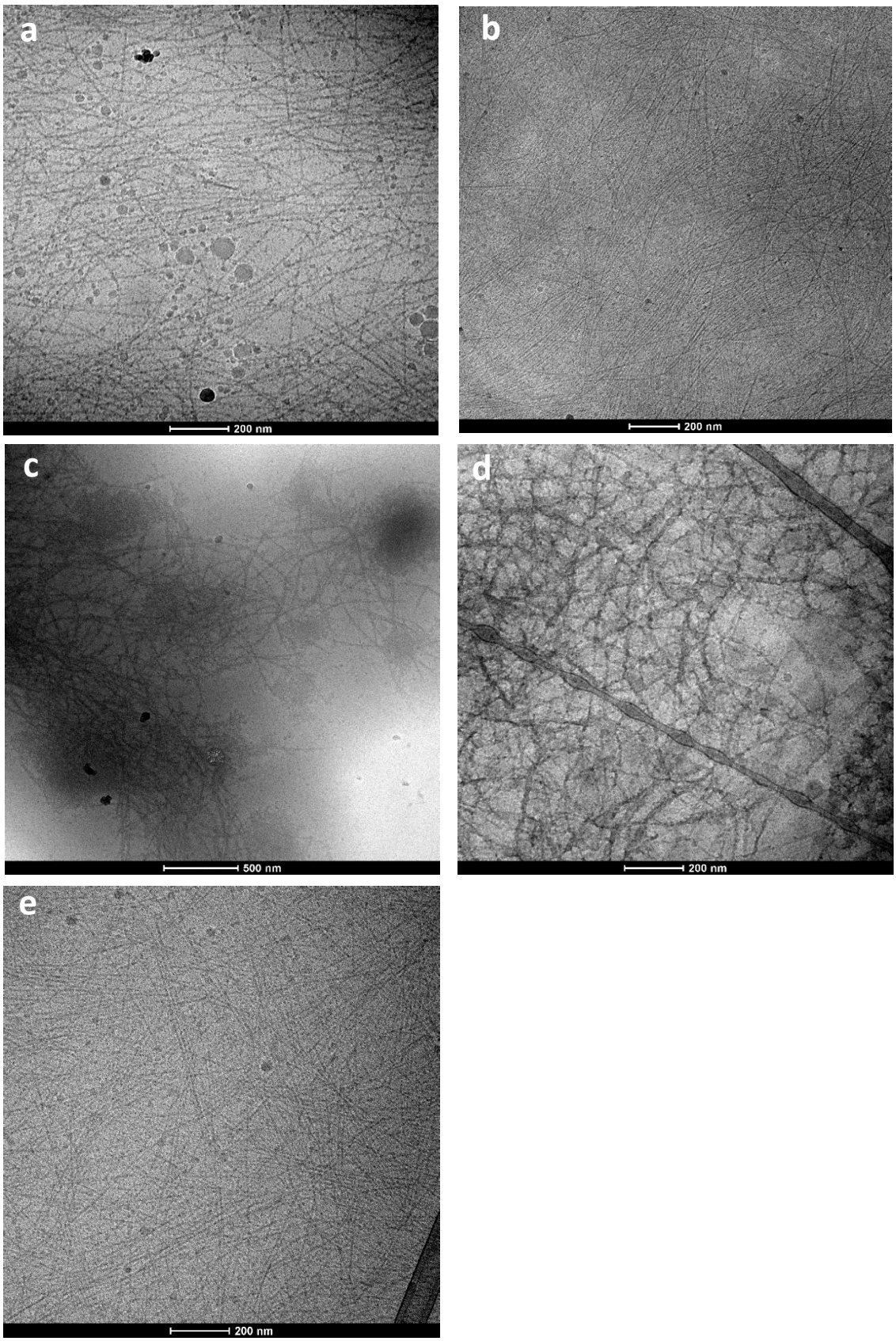

Fig. 14 Cryo-TEM images of dCPT-E_2(a), dCPT-OEG_2 (b),dCPT-KE (c) , dCPT-EK(d) and dCPT-OEG_2 after one month at a concentration of 200 uM in PBS with 50% human serum.

4. Conclusions

In summary, all designed drug amphiphiles with different chages are able to self assemble into nanotubes at a same condition, indicating that the self-assembly behaviors of these drug amphiphiles are dominated by the strong π-π interaction of CPT moieties in assembled form instead of the carrying charges. In addition, different degree of protein adsorption lead to the variations of stability of drug amphiphiles with different charges. Among all the molecules, cationic conjugates exihibited weakest stability while non-ionic drug amphiphiles are able to stable longest in biological environments. Thus, increasing the stability of drug amphiphile nanostructures in the precense of proteins can be achieved by incorporating OEG molecules into hydrophilic peptide sequences. We believe that this research provide a new platform for development of theranostic biodegradable nanostructures with a long retention time by reducing protein adsorption in human body.

References

1. Edwards, D.A., Hanes, J., Caponetti, G., J. Hrkach, BenJebria, A., M.L. Eskew, J. Mintzes, D. Deaver, N. Lotan, R. Langer, *Science*, 1997,276 1868–1871.
2. Kratz, F. *Journal of controlled release*, 2008,*132*(3), 171-183.
3. Chari, R. V., Miller, M. L., & Widdison, W. C., *Angewandte Chemie International Edition*, 2014, *53*(15), 3796-3827.
4. Su, H., Koo, J. M., & Cui, H., *Journal of Controlled Release*, 2015, *219*, 383-395.
5. Duncan, R., Vicent, M. J., Greco, F., & Nicholson, R. I., *Endocrine-related cancer*, 2005, *12*(Supplement 1), S189-S199.
6. Khandare, J., & Minko, T., *Progress in Polymer Science*, 2006, *31*(4), 359-397.
7. Lock, L. L., Tang, Z., Keith, D., Reyes, C., & Cui, H., *ACS Macro Letters*, 2015, *4*(5), 552-555..
8. Zhang, P., Cheetham, A. G., Lin, Y. A., & Cui, H., *Acs Nano*, 2013, *7*(7), 5965-5977.
9. Chen, Z., Zhang, P., Cheetham, A. G., Moon, J. H., Moxley, J. W., Lin, Y. A., & Cui, H., *Journal of Controlled Release*, 2014, *191*, 123-130.
10. Lock, L. L., Reyes, C. D., Zhang, P., & Cui, H., *Journal of the American Chemical Society*, 2016, *138*(10), 3533-3540.
11. Kang, M., Zhang, P., Cui, H., & Loverde, S. M., *Macromolecules*, 2016, *49*(3), 994-1001.
12. Su, H., Zhang, P., Cheetham, A. G., Koo, J. M., Lin, R., Masood, A., ... & Cui, H., *Theranostics*, 2016, *6*(7), 1065.
13. Lee, K. Y., & Mooney, D. J. *Chemical reviews*, 2011, *101*(7), 1869-1880.
14. Hamidi, M., Azadi, A., & Rafiei, P., *Advanced drug delivery reviews*,2008, *60*(15), 1638-1649.
15. Hoare, T. R., & Kohane, D. S., *Polymer*, 2008, *49*(8), 1993-2007.
16. Jeong, B., Kim, S. W., & Bae, Y. H., *Advanced drug delivery reviews*, 2002, *54*(1), 37-51.
17. Zhang, S.S., Fu, W.X. and Li, Z.B., *Polym. Chem.,* 2014, 5(10): 3346.
18. Srivastava, S., Andreev, M., Levi, A.E., Goldfeld, D.J., Mao, J., Heller, W.T., Prabhu, V.M., de Pablo, J.J. and Tirrell, M.V., Nat. Commun., 2017, 8: 14131.
19. Hoare, T.R. and Kohane, D.S., *Polymer*, 2008, 49(8): 1993.
20. Hartlieb, M., Kempe, K. and Schubert, U.S., *J. Mater. Chem*. B, 2015, 3(4): 526.
21. Patenaude, M., Smeets, N.M.B. and Hoare, T., *Macromol. Rapid Commun*., 2014, 35(6): 598.
22. Hennink, W.E. and van Nostrum, C.F., *Adv. Drug Deliver. Rev*., 2012, 64: 223.
23. Konieczynska, M.D. and Grinstaff, M.W*., Accounts Chem. Res*., 2017, 50(2): 151.
24. Holloway, J.L., Ma, H., Rai, R., Hankenson, K.D. and Burdick, J.A., *Macromol. Biosci.*, 2015, 15(9): 1218.
25. Khetan, S., Guvendiren, M., Legant, W.R., Cohen, D.M., Chen, C.S. and Burdick, J.A., *Nat. Mater*., 2013, 12(5): 458.
26. Rodell, C.B., Wade, R.J., Purcell, B.P., Dusaj, N.N. and Burdick, J.A*., ACS. Biomater. Sci. Eng.*, 2015, 1(4): 277.
27. Wade, R.J., Bassin, E.J., Rodell, C.B. and Burdick, J.A., *Nat. Commun*., 2015, 6: 6639.
28. Kloxin, A.M., Kasko, A.M., Salinas, C.N. and Anseth, K.S., *Science,* 2009, 324(5923): 59.
29. Brown, T.E., Marozas, I.A. and Anseth, K.S., *Adv. Mater*., 2017, 29(11): 1605001.
30. Grim, J.C., Marozas, I.A. and Anseth, K.S*., J. Control. Release*, 2015, 219: 95.
31. McKinnon, D.D., Brown, T.E., Kyburz, K.A., Kiyotake, E. and Anseth, K.S., *Biomacromolecules*, 2014, 15(7): 2808.

32. Rosales, A.M. and Anseth, K.S., *Nat. Rev. Mater*., 2016, 1(2): 15012.
33. Sridhar, B.V., Brock, J.L., Silver, J.S., Leight, J.L., Randolph, M.A. and Anseth, K.S., *Adv. Healthc. Mater*., 2015, 4(5): 702.
34. Du, X.W., Zhou, J., Shi, J.F. and Xu, B., *Chem. Rev*., 2015, 115(24): 13165.
35. Li, I.C., Moore, A.N. and Hartgerink, J.D., *Biomacromolecules*, 2016, 17(6): 2087.
36. Webber, M.J., Appel, E.A., Meijer, E.W. and Langer, R., *Nat. Mater*., 2016, 15(1): 13.
37. Sun, J.E.P., Stewart, B., Litan, A., Lee, S.J., Schneider, J.P., Langhans, S.A. and Pochan, D.J., *Biomater. Sci*., 2016, 4(5): 839.
38. Cui, H., Webber, M.J. and Stupp, S.I., *Biopolymers*, 2010, 94(1): 1.
39. Worthington, P., Langhans, S. and Pochan, D., *Adv. Drug Deliver. Rev*., 2017, 110-111: 127.
40. Moore, A.N. and Hartgerink, J.D., *Accounts Chem. Res*., 2017, 50(4): 714.
41. Berns, E.J., Sur, S., Pan, L.L., Goldberger, J.E., Suresh, S., Zhang, S.M., Kessler, J.A. and Stupp, S.I., *Biomaterials*, 2014, 35(1): 185.
42. Choe, S., Veliceasa, D., Bond, C.W., Harrington, D.A., Stupp, S.I., McVary, K.T. and Podlasek, C.A., *Acta Biomater*., 2016, 32: 89.
43. Acar, H., Srivastava, S., Chung, E.J., Schnorenberg, M.R., Barrett, J.C., LaBelle, J.L. and Tirrell, M., Adv. *Drug Deliver. Rev*., 2017, 110-111: 65.
44. Fleming, S. and Ulijn, R.V., *Chem. Soc. Rev.,* 2014, 43(23): 8150.
45. Raeburn, J. and Adams, D.J., *Chem. Commun*., 2015, 51(25): 5170.
46. Lock, L.L., Li, Y., Mao, X., Chen, H., Staedtke, V., Bai, R., Ma, W., Lin, R., Li, Y., Liu, G. and Cui, H., *ACS Nano*, 2017, 11(1): 797.
47. Su, H., Koo, J.M. and Cui, H., J. *Control. Release*, 2015, 219: 383.
48. Wang, Y., Cheetham, A.G., Angacian, G., Su, H., Xie, L. and Cui, H., *Adv. Drug Deliver. Rev*., 2017, 110-111: 112.
49. Chakroun, R.W., Zhang, P., Lin, R., Schiapparelli, P., Quinones-Hinojosa, A. and Cui, H., Wiley Interdiscip. *Rev. Nanomed. Nanobiotechnol*., 2017, DOI: 10.1002/wnan.1479.
50. Lock, L.L., LaComb, M., Schwarz, K., Cheetham, A.G., Lin, Y.A., Zhang, P. and Cui, H., *Faraday Discuss*., 2013, 166: 285.
51. Lin, R., Zhang, P., Cheetham, A.G., Walston, J., Abadir, P. and Cui, H., *Bioconjug. Chem.*, 2015, 26(1): 71.
52. Lock, L.L., Tang, Z., Keith, D., Reyes, C. and Cui, H., *ACS Macro Lett*., 2015, 4(5): 552.
53. Zhang, P., Lock, L.L., Cheetham, A.G. and Cui, H., *Mol. Pharm*., 2014, 11(3): 964
54. Cheetham, A.G., Zhang, P., Lin, Y.A., Lock, L.L. and Cui, H., *J. Am. Chem. Soc*., 2013, 135(8): 2907.
55. Su, H., Zhang, P., Cheetham, A.G., Koo, J.M., Lin, R., Masood, A., Schiapparelli, P., Quinones-Hinojosa, A. and Cui, H., *Theranostics*, 2016, 6(7): 1065.
56. Ma, W., Su, H., Cheetham, A.G., Zhang, W., Kan, Q. and Cui, H*., J. Control. Release,* 2017, DOI: 10.1016/j.jconrel.2017.01.015.
57. Su, H., Wang, Y., Anderson, C.F. et al. *Chin J Polym Sci* (2017) 35: 1194. https://doi.org/10.1007/s10118-017-1998-2.
58. Tenzer, S., Docter, D., Kuharev, J., Musyanovych, A., Fetz, V., Hecht, R., ... & Landfester, K. *Nature nanotechnology*, 2013, *8*(10), 772-781.
59. Cedervall, T., Lynch, I., Lindman, S., Berggård, T., Thulin, E., Nilsson, H., ... & Linse, S. *Proceedings of the National Academy of Sciences*, 2007,*104*(7), 2050-2055.
60. Monopoli, M. P., Åberg, C., Salvati, A., & Dawson, K. A. *Nature nanotechnology*, 2012, *7*(12), 779.
61. Aggarwal, P., Hall, J. B., McLeland, C. B., Dobrovolskaia, M. A., & McNeil, S. E. *Advanced drug delivery reviews*, 2009, *61*(6), 428-437.

62. Sacchetti, C., Motamedchaboki, K., Magrini, A., Palmieri, G., Mattei, M., Bernardini, S., ... & Bottini, M. *ACS nano*, 2013, *7*(3), 1974-1989.
63. Veronese, F. M., & Pasut, G. *Drug discovery today*, 2015, *10*(21), 1451-1458.
64. Alconcel, S. N., Baas, A. S., & Maynard, H. D. *Polymer Chemistry*, 2011, *2*(7), 1442-1448.
65. Baier, G., Baumann, D., Siebert, J. M., Musyanovych, A., Mailänder, V., & Landfester, K., *Biomacromolecules*, 2012, *13*(9), 2704-2715.
66. Landfester, K., & Mailänder, V., *Expert opinion on drug delivery*, 2013, *10*(5), 593-609.
67. Wörz, A., Berchtold, B., Moosmann, K., Prucker, O., & Rühe, J., *Journal of Materials Chemistry*, 2012, *22*(37), 19547-19561.
68. Otsuka, H., Nagasaki, Y., & Kataoka, K. (2012). *Advanced drug delivery reviews*, 2013, *64*, 246-255.
69. Del Pino, P., Pelaz, B., Zhang, Q., Maffre, P., Nienhaus, G. U., & Parak, W. J. *Materials Horizons*, 2014, *1*(3), 301-313.
70. Pelegri-O'Day, E. M., Lin, E. W., & Maynard, H. D.. *Journal of the American Chemical Society*, 2014,*136*(41), 14323-14332.Gr
71. ef, R., Lück, M., Quellec, P., Marchand, M., Dellacherie, E., Harnisch, S.,& Müller, R. H. *Colloids and Surfaces B: Biointerfaces*, 2000,*18*(3), 301-313.
72. Kim, H. R., Andrieux, K., Delomenie, C., Chacun, H., Appel, M., Desmaele, D., Electrophoresis 2017, 28, 2252–2261.
73. Storm, G., Belliot, S., Daemen, T., Lasic, D. D., Adv. Drug Deliv. Rev. 1995, 17, 31–48.
74. Peracchia, M. T., Vauthier, C., Desmaele, D., Gulik, A. et al., Pharm. Res. 1998, 15, 550–556.

YUZHU WANG

3400 North Charles Street, Baltimore, MD 21218, (443) 362-0913/ ywang287@jhu.edu

SUMMARY OF QUALIFICATIONS

Research experiences in studying the stability of self-assembling theranostic nanotubes in biological environments and developing antibody-purification immunofibers. Excel at laboratory management, training and project administration. Highly productive and efficient problem solver with a detail-oriented work style. Excellent writing skills and strong presentation abilities.

EDUCATION

- **M.S.**, Chemical and Biomolecular Engineering, Johns Hopkins University, Expected October 2017, GPA 3.75/4.0
  Thesis title: "Stability of Self-Assembling Drug Amphiphiles in Biological Environments"
  Advisor: Prof. Honggang Cui
- **B.S.**, Polymer Materials and Engineering, Beijing University of Chemical Technology, May 2015, GPA 3.62/4.0
  Thesis title: "Preparation and Characterization of Carboxylated Elastomer Graphene Oxidebiological Material"
  Advisor: Prof. Liqun Zhang

RELEVANT EXPERIENCE

Graduate Research Assistant **Nov. 2015-Present**
Johns Hopkins University, Department of Chemical and Biomolecular Engineering **Baltimore, MD**

- Developed a novel cost-efficient peptide-based platform technology for antibody purification using immunofibers with high antibody binding affinity and ease of handling; tested immunofibers binding affinity with IgG Fc3 with ITC. *(Collaborator: Bristol-Myers Squibb, 1 paper submitted to professional journal publication)*
- Designed and synthesized drug-peptide conjugates with different surface charges; characterized drug amphiphiles with HPLC, mass spectrometry, TEM, UV-Vis spectroscopy and circular dichroism; performed stability testing on pharmaceutical drug compounds in different biological environment; evaluated intracellular uptake and specific targeting with confocal microscopy and flow cytometry.
- Managed research projects with a team of 3 partners including: project management, planning, scheduling, inventory, purchasing, and equipment maintenance.
- Mentored 2 new research assistants on safety and lab techniques, resulting in no injuries or incidents, increased lab efficiencies and decreased re-work.
- Authored comprehensive reports on data findings, project analysis and project results, including professional journal publications.
- Held 2 poster presentations on 252nd American Chemical Society National Meeting & Exposition and 1 poster presentation on 14th International Nanomedicine & Drug Delivery Symposium.

Undergraduate Research Assistant **Nov. 2013-May. 2015**
Beijing University of Chemical Technology, Department of Materials Science and Engineering **Beijing, China**

- Created a composite of bio-based rubber and graphene with high strength, good air tightness, and high thermal and electrical conductivity.
- Synthesized biodegradable and linear poly(ester amide)s based on renewable resources. Investigated thermal stability, mechanical properties and in vitro degradation of produced poly(ester amide)s. *(1 paper published)*

SKILLS

- Research Skills: Peptide Synthesis, HPLC, MALDI-TOF, ESI Mass Spectrum, UV-Vis Spectrum, Fluorescence Spectrum, DSC, Dynamic Light Scattering, Small Angle X-ray Scattering, Circular Dichroism Spectroscopy, Optical Microscopy, TEM, ITC, Cell Culture
- Other Skills: Chemdraw, Origin, Adobe Photoshop, Adobe Illustrator, Word, Excel, PowerPoint

AWARDS AND RECOGNITIONS

- First Class Comprehensive Scholarship, BUCT, 2011
- Excellent Student Award, BUCT, 2012
- BASF Scholarship, BUCT,2013
- Second Prize in the National Science and Technology Innovation Competition, BUCT, 2014
- ChemBE Master's Essay Scholarship, JHU, 2016

PUBLICATIONS

- Bioinspired Supramolecular Engineering of Self-Assembling Immunofibers for High Affinity Binding of Immunoglobulin G, Yi Li, Lye Lin Lock, **Yuzhu Wang**, Xuankuo Xu, Zhengjian Li, Honggang Cui*, submitted to ACS Nano.
- Conformation Preservation of Alpha-Helical Peptides within Supramolecular Filamentous Assemblies, Yi Li, **Yuzhu Wang**, Shih-Hao Ou, Lye Lin Lock, Xuankuo Xu, Zhengjian Li, Honggang Cui*, Biomacromolecules, 2017, in press, DOI: 10.1021/acs.biomac.7b00992.
- Redox Sensitive Branched Nanostructure from Ferrocence Peptide Conjugated, Yin Wang, Hao Su, **Yuzhu Wang**, Honggang Cui*, submitted to Journal of the American Chemical Society.
- Mechanical Force Assisted Formation of Smaller Nanoobjects from Drug Amphiphiles, Yin Wang, Pengcheng Zhang, Ran Lin, Hao Su, **Yuzhu Wang**, Honggang Cui*, submitted to Journal of the American Chemical Society.
- Synergistic Antitumor Activity of Self-Assembling Camptothecin and Capecitabine Hybrid Prodrug for Improved Efficacy, Wang Ma[§], Hao Su[§], Andrew Cheetham, Weifang Zhang, **Yuzhu Wang**, Quancheng Kan, Honggang Cui*, Journal of Controlled Release, 2017, DOI: 10.1016/j.jconrel.2017.01.015.
- Recent Progress in Exploiting Small Molecule Peptides as Supramolecular Hydrogelators, Hao Su, **Yuzhu Wang**, Caleb Anderson, Jin Mo Koo, Chinese Journal of Polymer Science, 2017,35 (10), 1194-1211.
- Theranostic Biodegradable Nanotubes from Nanocovalent Prodrug Assemblys, Hao Su, Zhantong Wang, **Yuzhu Wang**, Jin Mo Koo, Xiaoyuan Chen*, Honggang Cui*, Manuscript in Preparation.
- Stability of Supramolecular Nanotubes in Biological Environment, **Yuzhu Wang**, Hao Su, Honggang Cui*, Manuscript in Preparation.
- One-Pot Synthesis of Biodegradable and Linear Poly(ester amide)s Based on Renewable Resources, Runguo Wang, Tiange Ren, Yunxiang Bai, **Yuzhu Wang**, Jianfeng Chen, Liqun Zhang*, Xiuying Zhao*, Journal of Applied Polymer Science, 2016, DOI: 10.1002/app.43446.

ACADEMIC PRESENTATIONS

- Supramolecular Assembly of Campothecin and Capecitabine Hybrid Drug Amphiphiles, Yuzhu **Wang**,Weifang Zhang, Hao Su, Wang Ma and Honggang Cui, 252nd ACS National Meeting & Exposition, Aug. 21-25, 2016, Philadelphia, PA, US. (Poster Presentation).
- Supramolecular Nanotubes by Anticancer Drug Assembly, Hao Su, **Yuzhu Wang**, Pengcheng Zhang, Jin Mo Koo, and Honggang Cui, 252nd ACS National Meeting & Exposition, Aug. 21-25, 2016, Philadelphia, PA, US. (Poster Presentation).
- Supramolecular Nanotubes by Anticancer Drug Assembly, Hao Su, **Yuzhu Wang**, Pengcheng Zhang, Jin Mo Koo, and Honggang Cui, 14th International Nanomedicine & Drug Delivery Symposium (NanoDDS'16), Sep. 16-18, 2016, Johns Hopkins University, Baltimore, MD, US. (Poster Presentation).